*Ann. Rev. Phys. Chem. 1984. 35 : 265–89*






# EFFECTS OF SATURATION ON LASER-INDUCED FLUORESCENCE MEASUREMENTS OF POPULATION AND POLARIZATION

*Robert Altkorn* and Richard N. Zare*

Department of Chemistry, Stanford University, Stanford, California 94305

## INTRODUCTION

This article addresses the effects of saturation in laser-induced fluorescence on both population and polarization measurements under certain conditions. Specifically, we examine low-pressure experiments in which collisional relaxation does not occur between excitation and detection. We use a rate equation approach to model the dynamics of spectroscopic transitions, and introduce directional Einstein coefficients to treat the interaction of a pulsed beam of polarized light with an anisotropic molecular distribution. There is an extensive body of literature related to saturation effects most of which concerns (*a*) optical pumping experiments, (*b*) laser physics, (*c*) high pressure studies, and (*d*) atomic systems. No attempt is made here to present a complete review of this field. Instead we cite mainly references that we feel would be of greatest relevance to workers applying LIF techniques to reaction dynamics.

### *Background*

The laser-induced fluorescence (LIF) technique has become a workhorse for detecting molecular species and determining their internal state

* Present address: Department of Chemistry, Northwestern University, Evanston, Illinois 60201.



0147–006X/84/0301–0265$02.00

distributions (1–5). It has been applied with advantage in various environments, from the ultra low pressure regimes of molecular beams and beam-surface scattering to the relatively high pressures of discharges (6) and flames (7). A great deal of attention has been concentrated on extracting relative populations from the variation of the fluorescence signal with wavelength (fluorescence excitation spectrum). Increasingly it has been realized that the accurate determination of relative populations requires an understanding of how the fluorescence signal varies with the polarization of the incident and detected photons (8, 9). Some polarization measurements are also interesting in their own right because they contain information about the anisotropy of the distribution of angular momentum vectors in the species being studied. In the past, workers using LIF to study reaction dynamics or molecular scattering assumed rather idealized conditions, in particular that the excited state population was strictly proportional to the laser intensity. This assumption fails as the laser power increases, and we refer to such nonlinear intensity-dependent behavior as *saturation*. Although the effects of saturation can be avoided in the limit of low laser power, in practice saturation effects are expected to be important, particularly when pulsed lasers are used.

Saturation effects were first observed in the radiofrequency (10, 11) and microwave (12–14) regimes, where excited state relaxation times are long and radiation sources of very high spectral brightness are common. As lasers were developed, saturation of molecular transitions with infrared radiation became possible (15, 16). With the advent of visible lasers, saturation effects were extended to include electronic transitions in atoms and molecules.

Nonlinear effects in optical pumping experiments have been treated in considerable generality and detail. Usually these experiments are not designed to measure the anisotropy or relative populations in a molecular distribution, but rather to determine atomic or molecular parameters such as Landé $g$ factors, excited state lifetimes, cross sections for energy transfer or depolarization, or various spectroscopic constants. Nevertheless, the theory developed for these experiments can also be applied to LIF measurements of the products of chemical reactions.

In a series of elegant papers (17–20), Ducloy discussed nonlinear behavior associated with the laser excitation of atoms or molecules in states of low (17, 18) or very large (classical limit) (19, 20) angular momenta. Ducloy's treatment assumes continuous-wave excitation and requires that a "broad line approximation" apply, in which the excitation probability is constant over the Doppler profile of the absorber. The excitation process is described in a density matrix formalism and the equations are solved

nonperturbatively. Ducloy allowed for the presence of an external field, arbitrary anisotropy in the molecular distribution, and excitation by linearly or circularly polarized light. This and other work on saturation effects in optical pumping experiments has been reviewed by Lehmann (21), Broyer et al (22), and Decomps, Dumont & Ducloy (23).

At the opposite extreme, a large amount of work has been done on the interaction of intense radiation with matter in the limit that the light source has infinitely narrow bandwidth, predominantly in connection with the theory of lasers (24–34). However, it is unlikely that this limit is reached in experiments using most pulsed tunable dye lasers. Behavior intermediate between the broad-line and infinitely narrow bandwidth limits is more complicated and has been discussed by Avan & Cohen-Tannoudji (35, 36).

The effect of saturation on LIF measurements conducted in the relatively high pressure regime has also been the subject of considerable effort. Most of the LIF measurements performed in this regime are designed to measure the temperature or concentration of various species in given portions of a flame or plasma. Piepmeier first suggested that saturation may actually prove beneficial in these measurements, pointing out that it could reduce the dependence of the fluorescence intensity on quenching rate (37, 38). This method was first applied to the detection of atoms in flames by Omenetto et al (39). Subsequently, a large number of saturated LIF measurements have been performed in the high pressure regime, the majority of which have involved the detection of atomic species. This work has been the subject of a number of reviews (7, 40–45). Saturated LIF experiments in flames have also been conducted with molecular species such as $C_2$ (46–48), CH (48, 49), CN (49), OH (43, 50–52), and MgO (53). This work has also been discussed in several reviews (7, 42–45).

Although the need for quenching rate data is minimized in saturated LIF measurements in flames, these experiments do have a number of complications. For example, the possibility of laser-induced chemistry (54–56) or ionization must be considered, complicated models must be used to take into account partial vibrational and rotational relaxation during the laser pulse (43, 57–60), and extrapolations to complete saturation must be carried out if only partial saturation can be achieved (47, 48). In addition, most models of saturation in flames have assumed that the collisional environment of atmospheric flames causes emission to be unpolarized. However, recent studies by Doherty & Crosley (61) have shown that this assumption need not hold.

Several groups have considered the effects of saturation on population measurements performed in the low pressure regime. These are inherently low-signal experiments because of the small concentrations of detected

species. Thus it might be desirable, or even necessary, to saturate the molecular transitions in order to obtain an acceptable fluorescence intensity. The importance of taking saturation into account has been emphasized by Allison, Johnson & Zare (62), who showed that saturation effects had caused a previous study of the $Ba + CF_3I$ reaction system (63) to be misinterpreted. Liu & Parson (64) and Córdova, Rettner & Kinsey (65) used rate equation models of the saturation process to aid in their analyses of data taken using tunable pulsed dye lasers. Neither group included polarization effects, although both groups, as well as Geraedts et al (66), pointed out that such effects should be taken into account. More recently, Guyer, Hüwel & Leone (67) reported LIF studies on $CO^+$ in which a strong saturation limit was achieved.

In addition to the previously mentioned work concerning optical pumping experiments and LIF studies in the low- and high-pressure regimes, the advent of the laser has motivated the study of saturation phenomena in a number of different areas. Just a few of these include the use of saturable absorbers as passive mode-locking devices in lasers (16, 68–71), work on saturation in semiconductors (72), and studies of saturation in inhomogeneously broadened laser gain media, especially concerning the Lamb dip (24, 73, 74). The Lamb dip provided perhaps the first of a large number of high-resolution spectroscopic methods falling under the general heading of saturation spectroscopy. The field of saturation spectroscopy has been reviewed in a number of books and articles (30, 75–79). A number of applications concern atomic systems, but saturation techniques can also be used to unravel complicated molecular spectra (80, 81).

## MODELING TRANSITION DYNAMICS

We use a rate equation approach to model the dynamics of spectroscopic transitions. Such an approach is justified when coherent transients (82–84) can be ignored. The suitability of rate equations for describing the interaction of laser light with atoms or molecules in the low pressure (collisionless) regime has been discussed by Cohen-Tannoudji (85), Avan & Cohen-Tannoudji (35), and Hertel & Stoll (86). These authors show that coherent effects can be neglected (*a*) if the coherence time of the laser (35, 85) is short compared to the pumping time (reciprocal of absorption or stimulated emission probability), or (*b*) the laser pulse is long compared to the excited-state radiative lifetime. How well these conditions are met depends on the type of laser used and the molecule being studied.

The second condition should easily be fulfilled if long-pulse (such as flashlamp-pumped) dye lasers are used to probe molecules with short

lifetimes. However, a situation in which the radiative lifetime is much longer than the laser pulse can occur if short-pulse (such as YAG-pumped) dye lasers are used to study molecules having long lifetimes (such as OH $A^2\Sigma^+$, which has a radiative lifetime of $\sim$700 ns, or NO $A^2\Sigma^+$ with a radiative lifetime of $\sim$180 ns).

Whether or not the first condition is met depends on the distribution of frequencies in the laser pulse. If the laser output consists of a very large number of closely spaced (overlapping) modes, the coherence time can be quite short. A long coherence time is obtained if the laser is run single mode and there are negligible fluctuations in the amplitude or phase of the laser output during the pulse. (This is probably best approximated by a pulse-amplified CW single-mode laser.)

Even if the experimenter is working in the limit at which coherent effects might manifest themselves, he/she must at least consider that:

1. The spatial profile of pulsed dye laser beams is usually quite inhomogeneous. Thus, there are regions of widely different intensity whose interactions with the molecules being probed must be averaged.
2. Dye lasers often have significant pulse-to-pulse intensity fluctuations. Because LIF measurements usually represent the average of a number of laser shots, again coherent transients are masked.

Thus it is likely that rate equations are adequate in most cases to calculate the effects of saturation on population and polarization measurements. When these assumptions break down, the optical Bloch equations (28, 29) still apply, but such studies commonly become more an investigation of the characteristics of the laser light source than of the atomic or molecular system under investigation (35).

## DIRECTIONAL EINSTEIN COEFFICIENTS

Rate equation models of spectroscopic transitions generally involve the Einstein $A$ and $B$ coefficients (87, 88). Implicit in the derivation of these quantities is an average over light of all directions and two orthogonal polarizations, as well as molecules of all orientations. Hence they are sometimes called the integrated Einstein coefficients. In LIF experiments, we are concerned with directional (polarized) radiation and molecular distributions that are often anisotropic. In order to treat the LIF process, we find it convenient to introduce the directional (or differential) Einstein coefficients, $a$ and $b$, which are used to model the interaction of directional, polarized radiation with molecules having a specific orientation. Although the directional Einstein coefficients are not widely known, they have been

discussed in detail by Stepanov & Gribkovskii (89). They may be defined in terms of the more familiar integrated Einstein coefficients by

$$a_{21} = \frac{8\pi^3\nu^3}{hc^3}|\mu_{12}|^2(\hat{\epsilon}\cdot\hat{\mu})^2 = \frac{3A_{21}}{8\pi}(\hat{\epsilon}\cdot\hat{\mu})^2 \quad 1.$$

and

$$b_{12} = b_{21} = \frac{8\pi^2}{h^2}|\mu_{12}|^2(\hat{\epsilon}\cdot\hat{\mu})^2 = 3B_{12}(\hat{\epsilon}\cdot\hat{\mu})^2, \quad 2.$$

where $(\hat{\epsilon}\cdot\hat{\mu})$ is the cosine of the angle between the electric field vector of the light and the transition dipole moment of the molecule and $|\mu_{12}|^2$ is the absolute square of the transition dipole between states 1 and 2 separated by the energy $h\nu$. It has also been assumed that states 1 and 2 have equal degeneracies. The factor of 1/3 in the relation between $b_{21}$ and $B_{21}$ arises from averaging $(\hat{\epsilon}\cdot\hat{\mu})^2$ over light of all directions and two orthogonal polarizations. The factor of $8\pi/3$ in the relation between $a_{21}$ and $A_{21}$ comes from integrating $(\hat{\epsilon}\cdot\hat{\mu})^2$ over an isotropic distribution of emitted light. We introduce the quantity $\rho(\nu, \Omega, \hat{\epsilon})$ as the density of radiation (energy per unit volume per unit frequency interval) directed into the solid angle $d\Omega$ whose electric field vector is specified by $\hat{\epsilon}$. Then, as shown in Figure 1, the rate of absorption of radiation characterized by $\rho(\nu, \Omega, \hat{\epsilon})d\Omega$ is given by

$$b_{12}\rho(\nu, \Omega, \hat{\epsilon})d\Omega N_1 \quad 3.$$

and the rate of emission of radiation having the same properties is given by

$$[b_{21}\rho(\nu, \Omega, \hat{\epsilon})d\Omega + a_{21}d\Omega]N_2. \quad 4.$$

Here $b_{12}$, $b_{21}$, and $a_{21}$ are the directional Einstein coefficients for absorption, stimulated emission, and spontaneous emission, respectively;

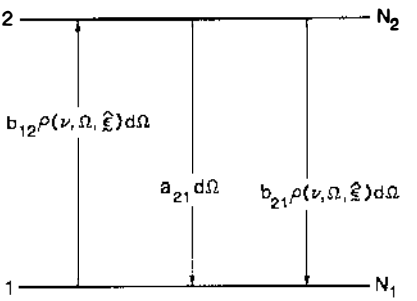


*Figure 1* Schematic diagram of a two-level system. The probability of absorption of light of frequency $\nu$ and polarization $\hat{\epsilon}$ directed into the solid angle $d\Omega$ is given by $b_{12}\rho(\nu, \Omega, \hat{\epsilon})d\Omega$. The probability of emission of light having the same properties is given by $b_{21}\rho(\nu, \Omega, \hat{\epsilon})d\Omega + a_{21}d\Omega$.

$N_1$ is the density of molecules in the lower state; and $N_2$ is the density of molecules in the excited state.

Before proceeding to describe LIF measurements in terms of the directional Einstein coefficients, we note the following points:

1. Molecular transitions have finite bandwidths and lasers often have sharp spectral mode structure. Implicit in the use of $b_{12}\rho(\nu, \mathbf{\Omega}, \hat{\varepsilon})d\mathbf{\Omega}$ for an absorption probability is the requirement that the laser output be effectively constant over the Doppler profile of the transition. If this is not the case, one must obtain an average absorption probability by integrating the mode structure of the laser over the bandwidth of the transition. As pointed out by Kinsey (2), if each of the modes is saturating a subset of molecules in a given velocity range, failing to perform this integration can introduce a significant error into the calculated absorption probability. Killinger, Wang & Hanabusa (51) have considered in some detail the effects of laser spectral profile on saturation behavior in the rate equation limit.

2. We have omitted $M$ sublevel degeneracy in discussing the directional Einstein coefficients. This is appropriate because the directional Einstein coefficients depend on the position of the transition dipole and therefore the $M$ sublevel. In practice, then, the experimenter must average the absorption probability over the anisotropy of the distribution. Our treatment applies to the large angular momentum limit when the $M$ level distribution can be approximated by a continuous function of the angle between the **J** vector and the axis of quantization.

3. We have chosen to describe the laser output in terms of its radiation density and have employed the cgs unit system. If one chooses for example to use the MKS system or to replace radiation density by intensity, slightly different formulae must be used for the Einstein coefficients. This has been discussed in detail by Hilborn (90).

## LASER-INDUCED FLUORESCENCE INTENSITY

Consider the experimental arrangement shown in Figure 2. This is the traditional excitation-detection geometry in which the laser is incident along the $X$ axis and linearly polarized along $\hat{\varepsilon}_a$ and fluorescence of linear polarization $\hat{\varepsilon}_d$ is collected in the $Y$ direction. For simplicity, we suppose that the molecular distribution is cylindrically symmetric about the $Z$ axis. This is the case, for example, in a beam-gas collision geometry when the beam is directed along the $Z$ axis or in a photodissociation experiment when the electric vector of the polarized photolysis beam is along the $Z$ axis.

The LIF measurement consists of two parts: We must first calculate the number of molecules excited by the laser and then the amount of

fluorescence incident on the detector. Initially, we consider only those molecules oriented such that $(\hat{\varepsilon}_a \cdot \hat{\mu})$ specifies the cosine of the angle between the transition dipole and the electric field vector of a laser. For these molecules, the excited state population is governed by the differential equation

$$\frac{dN_2}{dt} = N_1 b_{12}\rho(\nu, \Omega_a, \hat{\varepsilon}_a)d\Omega_a - N_2[A_{21} + b_{21}\rho(\nu, \Omega_a, \hat{\varepsilon}_a)d\Omega_a] \quad 5.$$

which is easily solved for a rectangular pulse of duration $\Delta t_L$ to yield

$$N_2 = \frac{Nb_{12}\rho(\nu, \Omega_a, \hat{\varepsilon}_a)d\Omega_a}{2b_{12}\rho(\nu, \Omega_a, \hat{\varepsilon}_a)d\Omega_a + A_{21}} \times \{1 - \exp[-(2b_{12}\rho(\nu, \Omega_a, \hat{\varepsilon}_a)d\Omega_a + A_{21})\Delta t_L]\}, \quad 6.$$

where $N = N_1 + N_2$ is the total concentration of the molecule in the state being probed. We have used $A_{21}$ rather than $a_{21}$ because the total rate at which the ground state is repopulated is of interest. We note that Eq. 5 is equivalent to that derived in the density matrix treatment in the limits of large angular momentum, broadband excitation, and no external fields (20–23).

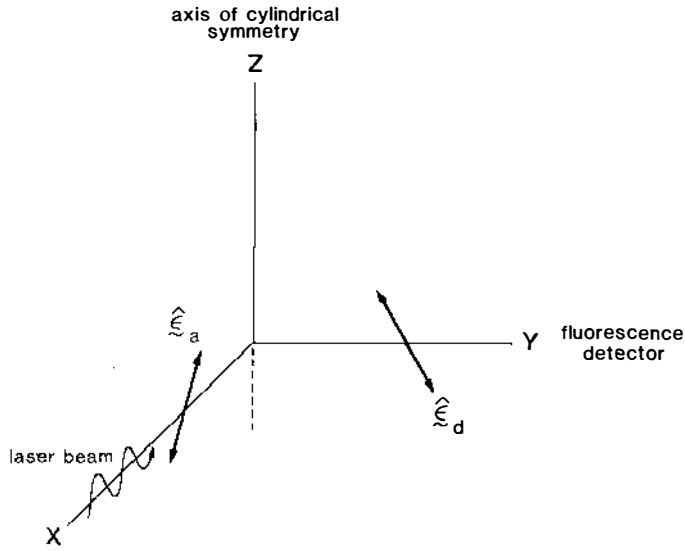


*Figure 2* Traditional right angle excitation-detection geometry. Molecules are excited by a laser of linear polarization $\hat{\varepsilon}_a$ incident along the $X$ axis. Fluorescence of linear polarization $\hat{\varepsilon}_d$ is detected along the $Y$ axis. The $Z$ axis is chosen to lie along the axis of cylindrical symmetry.

Having determined the number of molecules excited by the laser, we now consider the amount of fluorescence incident on the detector. The density of fluorescent radiation of polarization $\hat{\varepsilon}_d$ incident into the element of solid $d\Omega_d$ is given simply by $N_2 a_{21} d\Omega_d$. The intensity of detected fluorescence may be written as

$$I = K a_{21} N_2 \qquad 7.$$

where $K$ is a constant depending on the details of the detection system and $N_2$ is given by Eq. 6. Of course Eq. 7 applies only to those molecules oriented with a specific value of the cosine of the angle between the transition dipole and the electric field vector of the laser, given by $(\hat{\varepsilon}_a \cdot \hat{\mu})$ and a specific value of the cosine of the angle between the transition dipole and the electric vector of the detected fluorescence, given by $(\hat{\varepsilon}_d \cdot \hat{\mu})$. To obtain the total fluorescence intensity we must average over the entire distribution of molecules. In the classical limit, the molecular distribution is specified as $n(\theta)$ where $\theta$ is the angle between the **J** vector of the molecule and the $Z$ axis.

The position of the **J** vector can be related (8) to the position of the transition dipole $\boldsymbol{\mu}$ through

$$(\hat{\mu} \cdot \hat{\varepsilon})^2 = (\hat{\mathbf{J}} \cdot \hat{\varepsilon})^2 \qquad (Q \text{ branch}) \qquad 8.$$

and

$$(\hat{\mu} \cdot \hat{\varepsilon})^2 = \tfrac{1}{2}[1 - (\hat{\mathbf{J}} \cdot \hat{\varepsilon})^2] \qquad (P \text{ or } R \text{ branch}) \qquad 9.$$

for linearly polarized light. Substituting $n(\theta)$ for $N$ and using Eqs. 6 and 7, we obtain for the fluorescence intensity

$$I = K \int \frac{n(\theta) a_{21} b_{12} \rho}{2 b_{12} \rho + A_{21}} \times \{1 - \exp[-(2 b_{12} \rho + A_{21}) \Delta t_L]\} d\Omega \qquad 10.$$

where for convenience we write $\rho = \rho(\nu, \Omega_a, \hat{\varepsilon}_a) d\Omega_a$, $d\Omega$ is the solid angle element about **J**, and Eq. 8 or Eq. 9 must be substituted into Eq. 1 and Eq. 2 for $a_{21}$ and $b_{12}$. The angular dependence of $n(\theta)$ is commonly expressed through an expansion in Legendre polynomials:

$$n(\theta) = n \sum_{l=0}^{\infty} a_{2l} P_{2l} (\cos \theta) \qquad 11.$$

where $n$ represents the total concentration of molecules in the state of interest (assuming the normalization of $a_0 = 1$) and all odd moments are zero for a cylindrically symmetric distribution of **J** without handedness. (In any case only the even moments can be detected with linearly polarized

light.) Substituting Eq. 11 into Eq. 10, we obtain the grand result:

$$I = Kn \int \frac{\left( \sum_{l=0}^{\infty} a_{2l} P_{2l} (\cos \theta) \right) a_{21} b_{12} \rho}{2b_{12}\rho + A_{21}} \times \{1 - \exp[-(2b_{12}\rho + A_{21})\Delta t_L]\} d\Omega. \quad 12.$$

The above derivation is predicated on the following assumptions concerning the LIF experiment:

1. The experiment involves a pulsed laser and fluorescence is collected after the laser is off.
2. The laser pulse is perfectly uniform (although any coherent effects are assumed to be absent).
3. The solid angle subtended is sufficiently small so that $a_{21}$ is constant over the detector.
4. All states being studied have the same lifetime and quantum yield for fluorescence.
5. The LIF process in the atom or molecule can be accurately modeled using a two-level system (extension to a three-level system is considered in the Appendix).

Assuming that the laser pulse is perfectly uniform allows us to neglect any "hot spots" that might be present in the beam profile, the low-intensity wings of a Gaussian beam, and any intensity variations between the beginning and end of a pulse. Clearly, the experimenter may face the problem of saturating molecules with the more intense portions of the beam but obtaining linear behavior in regions of lower intensity. Thus Liu & Parson (64) and Córdova, Rettner & Kinsey (65) chose to measure a "saturation parameter" rather than use calculated values of the laser power and Einstein coefficients. We believe this procedure has much practical merit.

Effects due to a nonuniform beam profile have been considered by a number of workers, mostly in the field of flame and plasma diagnostics. Rodrigo & Measures (91) first pointed out that spatial inhomogeneity in the laser profile could cause the intensity actually needed to saturate a transition to be considerably higher than that calculated under the assumption of a homogeneous beam. Daily (92) analyzed the problem of saturating atoms in a flame with a Gaussian beam and came to a similar conclusion. Mailänder (48) discussed a method for determining a "saturated volume" throughout which the number of molecules in the excited state is constant. Van Calcar et al (93) have considered the importance of spatial beam profile in some detail. Using diaphragms and a diffuser to

improve the homogeneity of the laser beam, they report actual saturation behavior that agrees with their calculations to within 25% in studies of sodium atoms in flames. Van Calcar et al (94) also reported detailed studies of the spatial properties of a flashlamp-pumped dye laser beam.

In practice, the detector subtends a finite solid angle over which the fluorescence must be integrated. Usually the assumption is made that $a_{21}$ is constant over the detector. If this is not the case for a polarization experiment, a correction for finite solid angle must be included (95).

We also assume that all states being studied have the same lifetime. If this is not the case, it is important when interpreting the data to recognize that the populations of different excited states are decaying exponentially at different rates, and to integrate the expression for fluorescence intensity over the collection time. Alternatively, the experimenter may choose to collect fluorescence for a time long compared to the longest radiative lifetime, provided that the quantum yield is the same for all states. Then the fluorescence signal is once more proportional to the excited state population if the detector response is not biased by the rate of arrival of the fluorescent photons.

Finally, we turn to the assumption that the LIF process in the atom or molecule can be treated as a two-level system. If a short-pulse dye laser is being used, the laser is often on for a time $\Delta t_L$ much shorter than the excited state radiative lifetime $\tau$. Thus, spontaneous emission may be neglected during the excitation process, and a two-level system becomes appropriate. If the dye laser pulse is longer than the excited state radiation lifetime, a three-level system must be used to model the excitation process. A three-level system is straightforward but somewhat more complicated algebraically. We discuss such a treatment in the Appendix. The fluorescence process (after the laser is off) cannot in general be modeled by a two-level system as the atom or molecule usually radiates to a number of lower states. However, corrections for a three-level system are simple and also discussed in the Appendix.

## EFFECTS OF SATURATION ON POPULATION MEASUREMENTS

In the limit at which the exponential in Eq. 12 may be replaced by the first two terms in its Taylor series expansion

$$I = Kn\rho \int [1 + a_2 P_2 (\cos \theta) + a_4 P_4 (\cos \theta)] a_{21} b_{12} \Delta t_L d\Omega \qquad 13.$$

where terms containing Legendre polynomials of order greater than 4 have not been included because they vanish upon integration. This approximation is expected to be valid when the pumping rate is low (no saturation).

Using Eq. 1 and Eq. 2, we substitute $A_{21}$ and $B_{12}$ for $a_{21}$ and $b_{12}$ in Eq. 13 and obtain

$$I = \frac{9}{8\pi} Kn\rho A_{21} B_{12} \Delta t_L \int [1 + a_2 P_2 (\cos\theta) + a_4 P_4 (\cos\theta)] \times [\hat{\varepsilon}_a \cdot \hat{\mu}]^2 [\hat{\varepsilon}_d \cdot \hat{\mu}]^2 d\Omega. \quad 14.$$

Equation 14 can be further simplified if the following three conditions are satisfied:

1. The polarization of the laser and the detected fluorescence are unchanged during the experiment.
2. The distributions of molecules in all states probed by the laser are characterized by the same values of $a_2$ and $a_4$.
3. The fractions of collected fluorescence due to $Q$ branch and $P$ or $R$ branch transitions are the same for all states studied.

In this limit, the integral in Eq. 14 may be incorporated into the proportionality constant to give the familiar expression (2)

$$I = K' n B_{12} \rho \Delta t_L \quad 15.$$

where

$$K' = \frac{9}{8\pi} K A_{21} \int (1 + a_2 P_2 (\cos\theta) + a_4 P_4 (\cos\theta)) [\hat{\varepsilon}_a \cdot \hat{\mu}]^2 [\hat{\varepsilon}_d \cdot \hat{\mu}]^2 d\Omega. \quad 16.$$

It is Eq. 15 that is almost always assumed to be valid in extracting populations from LIF measurements. In order to compare the concentration of molecules in states $i$ and $j$, it is common (1) to form the ratio

$$\frac{n_i}{n_j} = \frac{I_i}{I_j} \frac{B_{12}^j \rho^j}{B_{12}^i \rho^i}. \quad 17.$$

(Here we have neglected any corrections due to changes in detector response with frequency.) Equation 15 is valid only in the limit of low laser power. As the laser power is increased, nonlinear behavior becomes apparent, and we must use the following expression, obtained from Eq. 12, to find $n_i/n_j$:

$$\frac{n_i}{n_j} = \frac{I_i \int \left[\sum_{l=0}^{\infty} a_{2l}^j P_{2l} (\cos\theta)\right] a_{21}^j b_{12}^j \rho^j \{1 - \exp[-(2b_{12}^j \rho^j + A_{21}^j)\Delta t_L]\} / (2b_{12}^j \rho^j + A_{21}^j) \, d\Omega}{I_j \int \left[\sum_{l=0}^{\infty} a_{2l}^i P_{2l} (\cos\theta)\right] a_{21}^i b_{12}^i \rho^i \{1 - \exp[-(2b_{12}^i \rho^i + A_{21}^i)\Delta t_L]\} / (2b_{12}^i \rho^i + A_{21}^i) \, d\Omega}. \quad 18.$$

There exists a limit in which Eq. 17 remains accurate for interpreting even saturated spectra. If the $b$ coefficients and the radiation density—as well as all angular factors—are the same for states $i$ and $j$, then both Eq. 17 and Eq. 18 reduce to

$$\frac{n_i}{n_j} = \frac{I_i}{I_j}. \qquad 19.$$

Thus in many practical cases, saturation should not change the appearance of LIF spectra. For example, such behavior might be expected for the members of a band progression ($\Delta v$ constant) in which the Franck-Condon factors are roughly all the same. In fact, saturation might be desirable in this case as it will increase the fluorescence signal. However, in probing features whose transition strengths differ significantly, saturation can seriously alter the appearance of the spectra. If this occurs, careful analysis is required to extract relative populations from the experimental data.

A dramatic example of the change in the appearance of a spectrum due to saturation is shown in Figure 3, taken by Allison, Johnson & Zare (62) with a maximum power of 5 MW/cm$^2$ in a 0.3 Å bandwidth. This spectrum includes $\Delta v = 0$ and $\Delta v = -1$ progressions of the $C^2\Pi_{3/2} - X^2\Sigma^+$ transition in BaI. It is seen that the $\Delta v = 0$ progression having large Franck-Condon factors "saturates first" and, as the laser power is increased, the members of the $\Delta v = -1$ progression increase in relative intensity. A change of about a factor of two occurs in the ratio of the $\Delta v = 0$ to $\Delta v = -1$ features when the laser power is attenuated by a factor of 100.

It is tempting to imagine that the experimenter can work in the limit of very strong saturation where simple expressions for the fluorescence intensity are recovered. In this case, conditions are such that $b_{12}\rho\Delta t_L \gg 1$ (and $b_{12}\rho \gg A_{21}$); hence Eq. 12 can be reduced to

$$I = \frac{Kn}{2} \int [1 + a_2 P_2 (\cos \theta)] a_{21} d\Omega. \qquad 20.$$

(Here terms containing Legendre polynomials of order greater than 2 integrate to zero.) We note that Eq. 20 is independent of the Einstein $B$ coefficients and laser power, because half of the molecules in the probed state are excited, regardless of their line strengths. Thus it becomes possible in principle to obtain relative populations or concentrations without knowledge of absorption line strengths! Unfortunately, this limit is difficult to achieve in practice, particularly with molecules. Some of the problems that must be confronted include (*a*) low-intensity wings of the laser beam and inhomogeneities in the beam profile, (*b*) the possibility of multiphoton processes as the laser intensity is increased, and (*c*) power restrictions of available dye lasers.

Nevertheless, some workers appear to have come very close to reaching

this limit. For example, in a particularly careful study, Van Calcar et al (93) were able to saturate sodium atoms in flames strongly with a flashlamp-pumped dye laser. They used a series of diaphragms to ensure that the flame was uniformly irradiated, and collected fluorescence from the uniformly irradiated volume during the high intensity portion of the laser pulse. Under these conditions, the fluorescence intensity increased very slowly as the laser power was raised. However, if the fluorescence was integrated over the low-intensity tail of the laser pulse, or if the beam was focused, it was much more difficult to reach the strong saturation limit.

Molecular transitions are more difficult to saturate than atomic transitions because they generally have considerably weaker absorption strengths. However, it appears possible to approach the strong saturation limit even if molecules are being studied. For example, in a study of OH in flames, Lucht, Sweeney & Laurendeau (43) found approximately equal

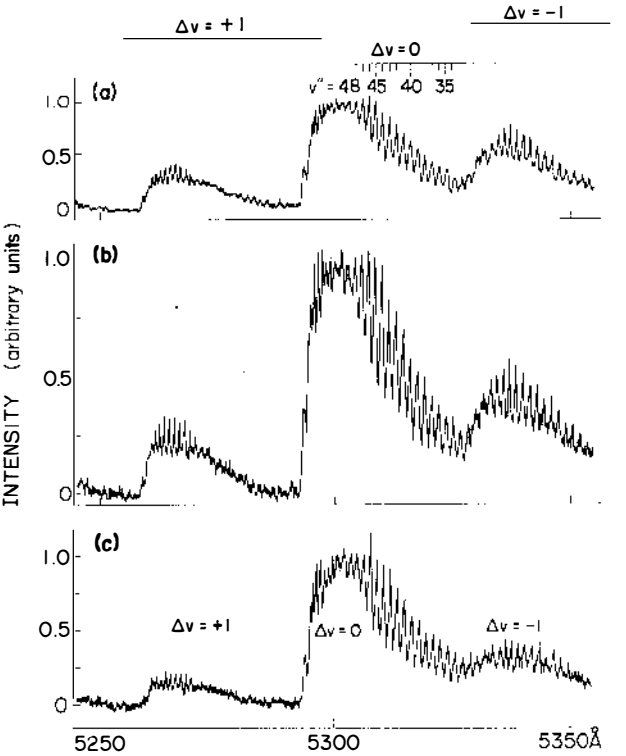


*Figure 3* Excitation spectra of BaI ($C^2\Pi_{3/2}-X^2\Sigma^+$) from the reaction $Ba+CF_3I$ obtained using (*a*) full laser power (5 MW/cm$^2$ over a 0.3 Å bandwidth), (*b*) one-tenth laser power, and (*c*) one-hundredth laser power. From Allison, Johnson & Zare (62).

fluorescence intensity from excitation by two peaks in the temporal output of a frequency-doubled YAG-pumped dye laser, even though the laser power in the two peaks differed by approximately a factor of two. (The fluorescence intensity dropped between the peaks, apparently due to collisional deexcitation of OH.)

## EFFECT OF SATURATION ON POLARIZATION MEASUREMENTS

Polarization measurements are designed to obtain information about the distribution of angular momentum vectors in an atomic or molecular ensemble. When discussing polarization measurements in the absence of saturation, we are again interested in Eq. 14, which we rewrite (to consolidate as many constants as possible) as

$$I = K'' \int (1 + a_2 P_2 (\cos\theta) + a_4 P_4 (\cos\theta)) [\hat{\epsilon}_a \cdot \hat{\mu}]^2 [\hat{\epsilon}_d \cdot \hat{\mu}]^2 d\Omega \qquad 21.$$

where

$$K'' = \frac{9}{8\pi} K n \rho A_{21} B_{12} \Delta t_L. \qquad 22.$$

In principle, it is possible to obtain $a_2$ and $a_4$ by performing four LIF measurements on the molecular ensemble (8, 9, 96). The four measurements usually involve polarizing the laser along each of the $Z$ and $Y$ axes and collecting fluorescence polarized along each of the $Z$ and $X$ axes. The fluorescence intensities for each of the four excitation geometries and the four possible combinations of $Q$ and $P$ or $R$ branch transitions are listed in Table 1.

**Table 1** The fluorescence signal $I(a_2, a_4)$ obtained from a cylindrical molecular distribution[a] $n(\theta)$ for different resonance fluorescence branches

| Excitation-detection polarization | | Branch type[b] | | | |
|---|---|---|---|---|---|
| $\hat{\epsilon}_a$ | $\hat{\epsilon}_d$ | ($P$ or $R\uparrow$, $P$ or $R\downarrow$) | ($Q\uparrow$, $Q\downarrow$) | ($P$ or $R\uparrow$, $Q\downarrow$) | ($Q\uparrow$, $P$ or $R\downarrow$) |
| $\hat{Z}$ | $\hat{Z}$ | $168-48a_2+8a_4$ | $252+144a_2+32a_4$ | $84+12a_2-16a_4$ | $84+12a_2-16a_4$ |
| $\hat{Z}$ | $\hat{X}$ | $126-18a_2-4a_2$ | $84+12a_2-16a_2$ | $168-48a_2+8a_4$ | $168+78a_2+8a_4$ |
| $\hat{Y}$ | $\hat{Z}$ | $126-18a_2-4a_4$ | $84+12a_2-16a_4$ | $168+78a_2+8a_4$ | $168-48a_2+8a_4$ |
| $\hat{Y}$ | $\hat{X}$ | $126+36a_2+a_4$ | $84-24a_2+4a_4$ | $168-30a_2-2a_4$ | $168-30a_2-2a_4$ |

[a] $n(\theta)$ has the form $\sum_l a_{2l} P_{2l}$ (cos $\theta$) where $a_0 = 1$; only the $a_2$ and $a_4$ coefficients can be determined by the measurements.

[b] All entries should be multiplied by $\pi K''/315$.

In the limit of very strong saturation, Eq. 20 again becomes applicable. In this case the probability of exciting a molecule is independent of its orientation or the polarization of the laser. The analysis of the LIF experiment then becomes equivalent to that of an excited-state emission experiment (97, 98), only permitting the determination of $a_2$. The intensities of $Z$ and $X$ polarized fluorescence due to $Q$ and $P$ or $R$ branch transitions in the strong saturation limit are shown in Table 2.

Between the unsaturated and strongly saturated limits, Eq. 12 relates LIF measurements to moments of the molecular distribution. We have written a computer program to evaluate Eq. 12. In Figure 4 we show calculated fluorescence polarizations ($P = [I_Z - I_X]/[I_Z + I_X]$) for measurements involving ($P$ or $R\uparrow$, $P$ or $R\downarrow$) and ($Q\uparrow, Q\downarrow$) transitions, respectively. The fluorescence polarization is displayed as a function of the reduced absorption probability, $D$, where

$$D = b_{12}\rho\Delta t_L/[\hat{\varepsilon}_a \cdot \hat{\mu}]^2. \qquad 23.$$

(The absorption probability is given by $D[\hat{\varepsilon}_a \cdot \hat{\mu}]^2$.) We have assumed the laser to be polarized along the $Z$ axis and have evaluated Eq. 12 for the following molecular distributions:

1. isotropic ($a_0 = 1$);
2. $\sin^2\theta$ distribution ($a_0 = 1, a_2 = -1$);
3. $\cos^2\theta$ distribution ($a_0 = 1, a_2 = 2$);
4. pure quadrupole distribution ($a_0 = 1, a_4 = -1$); and
5. pure hexadecapole distribution ($a_0 = 1, a_6 = -1$). (In distributions 1–5, $a_n = 0$ for all $a_n$ not specified.)

It is seen that between the unsaturated and strongly saturated limits, the fluorescence intensity is dependent on $a_6$ for the distributions considered in Figures 4a and 4b. In general the fluorescence intensity in the moderately

**Table 2** The fluorescence signal $I(a_2)$ obtained from a cylindrical molecular distribution[a] $n(\theta)$ for different fluorescence branches in the strong saturation limit

| Detection polarization | Branch type[b] | |
|---|---|---|
| $\hat{\varepsilon}_d$ | $P$ or $R$ | $Q$ |
| $\hat{Z}$ | $10-2a_2$ | $10+4a_2$ |
| $\hat{X}$ | $10+a_2$ | $10-2a_2$ |

[a] $n(\theta)$ has the form $\sum_l a_{2l}P_{2l}(\cos\theta)$ where $a_0 = 1$; only the $a_2$ coefficients can be determined by the measurements.
[b] All entries should be multiplied by $KnA_{21}/40$.

saturated regime depends on all higher-order even moments of the distribution. This opens in principle the possibility of detecting these higher-order moments, although their quantitative determination is at best problematic.

It is also evident from comparing Figures 4a and 4b that the polarizations involving $(Q\uparrow, Q\downarrow)$ transitions seem to converge to the strongly

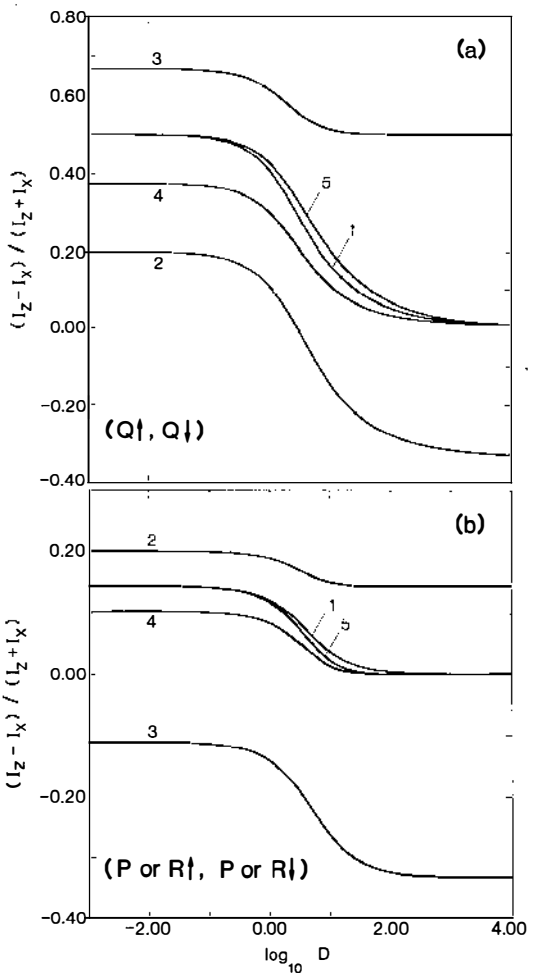


*Figure 4* Calculated change in polarization vs the logarithm of the reduced absorption probability $D$ for five molecular **J** vector distributions. The distributions are as follows: 1. isotropic ($a_0 = 1$); 2. $\sin^2\theta$ ($a_0 = 1, a_2 = -1$); 3. $\cos^2\theta$ ($a_0 = 1, a_2 = 2$); 4. pure quadrupole ($a_0 = 1, a_4 = -1$); 5. pure hexadecapole ($a_0 = 1, a_6 = -1$). Here (*a*) refers to excitation and fluorescence via $Q$ branches, and (*b*) via $P$ or $R$ branches.

saturated limit much more slowly than do those involving ($P$ or $R\uparrow$, $P$ or $R\downarrow$) transitions. This follows from the fact that $Q$ branch transition dipoles lie along the **J** vector and undergo no spatial averaging as the molecule rotates. Thus, exciting with a $Z$-polarized laser and collecting $X$-polarized fluorescence sets up a situation in which the molecules that contribute the most fluorescence intensity are the most difficult to saturate because of the angular term in the $b$ coefficient.

## ROLE OF ANGULAR FACTORS IN SATURATION BEHAVIOR

Our treatment of saturation differs from previous work (64, 65) in that we include explicitly the dependence of fluorescence intensity on the excitation-detection geometry, including the type ($P$, $R$ or $Q$) of resonance fluorescence branches, the polarization of the absorbed and detected photons, and the (possible) anisotropy of the ensemble of absorbing species. It is useful to determine whether this treatment involving angular factors, such as directional Einstein coefficients, may be replaced by a treatment involving simply the integrated Einstein coefficients. To explore the adequacy of this simpler approximation, we have plotted in Figure 5 the fluorescence intensity arising from an isotropic distribution of absorbers against the reduced absorption probability, $D$. We assume the traditional excitation-detection geometry of Figure 2, and we consider the incident light to be linearly polarized. We plot $I_{\parallel}$ corresponding to $\hat{\boldsymbol{\varepsilon}}_a \parallel \hat{\boldsymbol{\varepsilon}}_d$, $I_{\perp}$ corresponding to $\hat{\boldsymbol{\varepsilon}}_a \perp \hat{\boldsymbol{\varepsilon}}_d$, and their average value, $(I_{\parallel} + I_{\perp})/2$, for both ($Q\uparrow$,$Q\downarrow$) and ($P$ or $R\uparrow$, $P$ or $R\downarrow$) transitions. We also show by a dotted line the result when $[\hat{\boldsymbol{\varepsilon}} \cdot \hat{\boldsymbol{\mu}}]^2$ is replaced by its average value of one-third, and the fluorescence intensity is normalized to have the same maximum value at infinite laser power as in the other three cases. This procedure is equivalent to using integrated Einstein coefficients (see Eq. 2).

Figure 5 shows the existence of three intensity regimes. The first is a linear dependence at low laser power (see insets); the second regime occurs at intermediate laser power and is characterized by strong nonlinear dependence of the fluorescence intensity on $D$; and the third regime is once again linear with almost zero slope at high laser power. The onsets of these three regimes occur at different laser powers for $I_{\parallel}$ and $I_{\perp}$. Indeed, $I_{\parallel}$ begins to exhibit nonlinear behavior with laser power at lower power levels than $I_{\perp}$. Moreover, $I_{\parallel}$ much more rapidly reaches the strongly saturated regime than $I_{\perp}$. It is a matter of much practical concern to test for saturation effects. Clearly, the (linear) variation of fluorescence signal with laser power is the most straightforward diagnostic. Figure 5 shows that the measurement of $I_{\parallel}$ is the most sensitive way of carrying out this test. Conversely, if the

experimenter wishes to achieve the strongly saturated limit, the observation of $I_{\parallel}$ is again to be commended.

Figure 5 also shows that $(I_{\parallel} + I_{\perp})/2$ is extremely well approximated by the calculation of saturation effects based on the integrated Einstein coefficients (46, 47), at least for low and intermediate laser power levels. This conclusion justifies the previous neglect of angular factors in calculating the behavior of fluorescence intensity with laser power for isotropic distributions, but cannot be expected to hold for nonisotropic distributions.



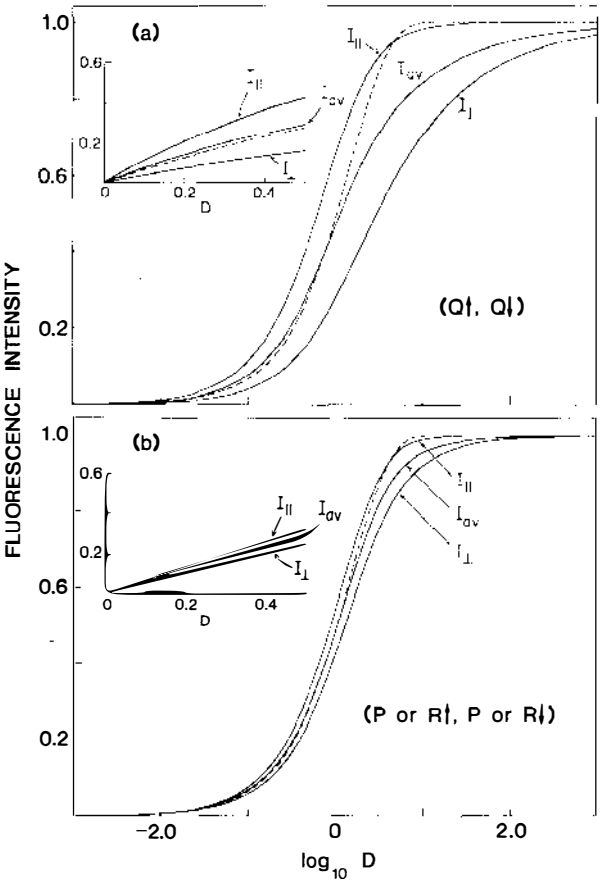


*Figure 5* Fluorescence intensity versus reduced absorption probability: (*a*) for $(Q\uparrow, Q\downarrow)$ transitions, and (*b*) for ($P$ or $R\uparrow$, $P$ or $R\downarrow$) transitions. The *solid lines* are $I_{\parallel}$, $I_{\perp}$, and $I_{av} = (I_{\parallel} + I_{\perp})/2$; the *dotted line* is a calculation based on integrated Einstein coefficients. All curves are normalized to unit value at infinite laser power.

## USING SATURATION TO MEASURE FLUX—A SPECIAL CASE

The measurement of reaction rates or cross sections requires a knowledge of product flux (the number of molecules crossing a unit area in a unit time, or equivalently, the density of molecules multiplied by their velocity). However, LIF usually functions as a density detector (99). An important question is whether saturation can transform the LIF technique from a density to a flux detector. Unfortunately the answer is seldom in the affirmative.

Using the first definition of flux given above, we see that in order for a laser to detect flux it must effectively define a surface and excite molecules that cross that surface with a probability that is independent of molecular velocity. For this condition to be fulfilled, the number of molecules that pass through the beam while it is on must be much greater than the number of molecules present in the beam at any instant. This is clearly not the case in most experiments involving short-pulse dye lasers. The diameter of an average pulsed laser beam is much greater than the distance moved by most chemical reaction products in the time during which a short-pulse laser is on. Thus the molecules are stationary on the time scale of the laser pulse and the laser must rigorously function as a density detector (although in special circumstances, density and flux detection could be equivalent). On the other hand, a CW laser might be used as a flux detector (100) if the strong saturation limit were achieved and the excited molecules did not return to a state that can reabsorb the laser radiation. Then each molecule passing through the laser beam can be detected once and only once in principle. Often the situation is much more complicated and something between flux and density is measured. In a different scheme, a laser might be used under some conditions to measure the density and velocity simultaneously, for example through the Doppler shift (101–104) or through "hole burning" (104, 105), and thereby allow flux to be determined.

## SUMMARY

Experimental and theoretical studies of saturation effects on resonance fluorescence have been briefly reviewed. We have restricted our attention to molecules in a collisionless environment excited by pulsed laser sources. In the limit of large rotational angular momentum, directional Einstein coefficients were introduced and rate equations developed to describe the fluorescence intensity as a function of both laser and fluorescence polarization for linearly polarized light interacting with a cylindrically symmetric molecular distribution.

Saturation may actually prove beneficial in some population measure-

ments. This can occur if the strengths of all the transitions composing the spectrum are approximately the same. In this case saturation will not significantly alter the appearance of the spectrum but it may improve signal to noise. If the transition strengths differ greatly, however, saturation can significantly distort the appearance of the spectrum. On the other hand, saturation is rarely advantageous in polarization measurements. In these experiments a "spectrum" is obtained not by scanning wavelength but by varying the polarization of the incident and/or detected light. As the polarization is varied, molecules having different orientations and therefore different transition strengths due to angular factors are selectively detected, and the "spectrum" must change with saturation. In moderately saturated regimes, the fluorescence intensity depends on higher orders of the molecular distribution, making polarization data difficult to invert. In the strongly saturated limit, only the second Legendre moment of the angular momentum distribution is obtainable, whereas in unsaturated measurements both the second and fourth moments are accessible to study.



## ACKNOWLEDGMENTS

We thank the many people who read earlier drafts of this manuscript and offered suggestions for its improvement. In particular, we are especially grateful to Klaas Bergmann, Paul J. Dagdigian, James DeHaven, Mark A. Johnson, Stephen R. Leone, Guang Hai Lin, Kopin Liu, John McKillop, John M. Parson, Charles T. Rettner, Thomas Trickl, and Jochen Wanner for their assistance. This work was supported by the National Science Foundation. R. N. Z. gratefully acknowledges support through the Shell Distinguished Chairs Program, funded by Shell Companies Foundation, Inc.

## APPENDIX

We consider here the use of a three-level system, shown in Figure 6, for modeling the LIF process. We assume that the laser is resonant on the transition between states 1 and 2. The excited state can radiate to a number of states other than state 1. We call these collectively state 3 and assume that they are not connected to the ground state on the time scale of the laser pulse, $\Delta t_L$. The populations evolve according to the coupled differential equations

$$\frac{dN_1}{dt} = -b_{12}\rho N_1 + (b_{21}\rho + A_{21})N_2 \qquad \text{A-1.}$$

$$\frac{dN_2}{dt} = b_{12}\rho N_1 - (b_{21}\rho + \tau^{-1})N_2 \qquad \text{A-2.}$$

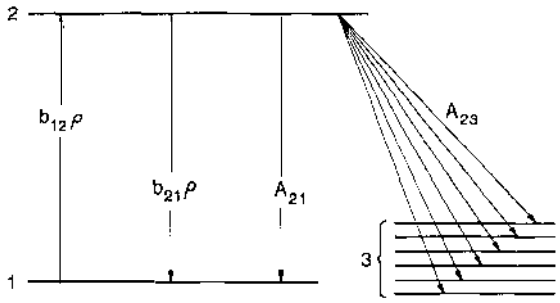


*Figure 6* Schematic diagram of a three-level system. All ground state levels other than that being pumped are grouped together as level 3. The probability of exciting a molecule oriented such that $(\hat{\varepsilon}\cdot\hat{\mu})$ is the cosine of the angle between the electric vector of the light and the transition dipole is given by $b_{12}\rho$. The total probability of emission from excited molecules having the same orientation is given by $b_{21}\rho + A_{21} + A_{23}$.

where $\tau$ is the lifetime of state 2. The population of state 3 follows by subtraction from the total concentration of molecules, $N$. Equations A-1 and A-2 may be solved to yield

$$N_2 = \frac{b_{12}\rho N(e^{\lambda_1 \Delta t_L} - e^{\lambda_2 \Delta t_L})}{\lambda_1 - \lambda_2} \qquad \text{A-3.}$$

and

$$N_1 = \frac{N[(b_{12}\rho + \tau^{-1} + \lambda_1)e^{\lambda_1 \Delta t_L} - (b_{12}\rho + \lambda_2 + \tau^{-1})e^{\lambda_2 \Delta t_L}]}{\lambda_1 - \lambda_2} \qquad \text{A-4.}$$

where $N$ is the total number of atoms or molecules, and $\lambda_1$ and $\lambda_2$ are given by

$$\lambda_{1,2} = \tfrac{1}{2}\{-2b_{12}\rho - \tau^{-1} \pm (\tau^{-2} + 4b_{12}\rho A_{21} + 4b_{12}{}^2\rho^2)^{1/2}\}. \qquad \text{A-5.}$$

The three-level system described here has been used previously by Córdova, Rettner & Kinsey (65) (neglecting polarization effects) in their study of OH. A more general description of three-level systems as well as a discussion of systems with arbitrary numbers of energy levels is given by Stepanov & Gribkovskii (89).

If a three-level system must be used to describe the excitation process, Eq. 12 should be replaced by

$$I = Kn \int \frac{\left[\sum_{l=0}^{\infty} a_{2l} P_{2l}(\cos\theta)\right] b_{12}\rho(e^{\lambda_1 \Delta t_L} - e^{\lambda_2 \Delta t_L})(a_{21} + a_{23})\mathrm{d}\Omega}{\lambda_1 - \lambda_2}. \qquad \text{A-6.}$$

If a two-level system is adequate to model the excitation process, but a three-level system is necessary to describe fluorescence, $a_{21} + a_{23}$ should be substituted for $a_{21}$ in Eq. 12.

*Literature Cited*


1. Zare, R. N., Dagdigian, P. J. 1974. *Science* 185:739–47
2. Kinsey, J. L. 1977. *Ann. Rev. Phys. Chem.* 28:349–72
3. Levy, M. R. 1979. *Progr. React. Kinet.* 10:1–252
4. Clyne, M. A. A., McDermid, I. S. 1982. *Dynamics of the Excited State, Adv. Chem. Phys.*, ed. K. P. Lawley, 50:1–104
5. Bernstein, R. B. 1982. *Chemical Dynamics via Molecular Beam and Laser Techniques.* Oxford: Clarendon. 262 pp.
6. Gottscho, R. A., Miller, T. A. 1984. *Pure Appl. Chem.* 56:189–208
7. Crosley, D. R., ed. 1980. *Laser Probes for Combustion Chemistry*, ACS Symp. Ser. 134. Washington DC: Am. Chem. Soc. 495 pp.
8. Case, D. A., McClelland, G. M., Herschbach, D. R. 1978. *Mol. Phys.* 35:541–73
9. Greene, C. H., Zare, R. N. 1983. *J. Chem. Phys.* 78:6741–53
10. Abragam, A. 1961. *The Principles of Nuclear Magnetism.* Oxford: Clarendon. 599 pp.
11. Slichter, C. P. 1978. *Principles of Magnetic Resonance.* New York: Springer. 397 pp. 2nd ed.
12. Townes, C. H. 1946. *Phys. Rev.* 70:665–71
13. Karplus, R., Schwinger, J. 1948. *Phys. Rev.* 73:1020–26
14. Karplus, R. 1948. *Phys. Rev.* 74:223–24
15. Burak, I., Steinfeld, J. I., Sutton, D. G. 1969. *J. Quant. Spectrosc. Radiat. Transfer* 9:959–80
16. Giuliano, C. R., Hess, L. D. 1967. *IEEE J. Quant. Elec.* QE-3:358–67
17. Ducloy, M. 1973. *Phys. Rev. A* 8:1844–59
18. Ducloy, M. 1974. *Phys. Rev. A* 9:1319–42
19. Ducloy, M. 1975. *J. Phys.* 36:927–41
20. Ducloy, M. 1976. *J. Phys. B* 9:357–81
21. Lehmann, J. C. 1977. *Les Houches Session XXVII, Frontiers in Laser Spectroscopy*, ed. R. Balian, S. Haroche, S. Liberman, pp. 475–527. Amsterdam: North Holland
22. Broyer, M., Gouedard, G., Lehmann, J. C., Vigué, J. 1976. *Adv. At. Mol. Phys.* 12:165–213
23. Decomps, B., Dumont, M., Ducloy, M. 1976. *Topics in Applied Physics, Vol. 2, Laser Spectroscopy of Atoms and Molecules*, ed. H. Walther, pp. 283–347. New York: Springer
24. Lamb, W. E. Jr. 1964. *Phys. Rev.* 134: A1429–50
25. Stenholm, S., Lamb, W. E. Jr. 1969. *Phys. Rev.* 181:618–35
26. Feldman, B. J., Feld, M. S. 1970. *Phys. Rev. A* 1:1375–96
27. Holt, H. K. 1970. *Phys. Rev. A* 2:233–49
28. Sargent, M. III, Scully, M. O., Lamb, W. E. Jr. 1974. *Laser Physics.* Reading, Mass: Addison-Wesley. 432 pp.
29. Allen, L., Eberly, J. H. 1975. *Optical Resonance and Two Level Atoms.* New York: Wiley-Interscience. 233 pp.
30. Letokhov, V. S., Chebotayev, V. P. 1977. *Nonlinear Laser Spectroscopy.* Berlin: Springer-Verlag. 466 pp.
31. Smith, R. A. 1978. *Proc. R. Soc. London Ser. A* 362:1–12
32. Smith, R. A. 1978. *Proc. R. Soc. London Ser. A* 362:13–25
33. Smith, R. A. 1979. *Proc. R. Soc. London Ser. A* 368:163–75
34. Smith, R. A. 1980. *Proc. R. Soc. London Ser. A* 371:319–29
35. Avan, P., Cohen-Tannoudji, C. 1977. *J. Phys. B* 10:155–70
36. Avan, P., Cohen-Tannoudji, C. 1977. *J. Phys. B* 10:171–85
37. Piepmeier, E. H. 1972. *Spectrochim. Acta B* 27:431–43
38. Piepmeier, E. H. 1972. *Spectrochim. Acta B* 27:445–52
39. Omenetto, N., Bennetti, P., Hart, L. P., Winefordner, J. D., Alkemade, C. Th. J. 1973. *Spectrochim. Acta B* 28:289–300
40. Winefordner, J. D., Omenetto, N. 1979. *Analytical Laser Spectroscopy*, ed. N. Omenetto, pp. 167–218. New York: Wiley
41. Winefordner, J. D. 1978. *New Applications of Lasers to Chemistry*, ACS Symp. Ser. 85, ed. G. M. Hieftje, pp. 50–79. Washington DC: Am. Chem. Soc.
42. Eckbreth, A. C., Bonczyk, P. A., Verdieck, J. F. 1977. *Appl. Spectrosc. Rev.* 13:15–164
43. Lucht, R. P., Sweeney, D. W., Lauren-

deau, N. M. 1983. *Combust. Flame* 50:189–205
44. Schofield, K., Steinberg, M. 1981. *Opt. Eng.* 20:501–10
45. Crosley, D. R. 1981. *Opt. Eng.* 20:511–21
46. Baronavski, A. P., McDonald, J. R. 1977. *J. Chem. Phys.* 66:3300–1
47. Baronavski, A. P., McDonald, J. R. 1977. *Appl. Opt.* 16:1897–1901
48. Mailänder, M. 1978. *J. Appl. Phys.* 49: 1256–59
49. Bonczyk, P. A., Shirley, J. A. 1979. *Combust. Flame* 34:253–64
50. Takubo, Y., Yano, H., Matsuoka, H., Shimazu, M. 1983. *J. Quant. Spectrosc. Radiat. Transfer* 30:163–68
51. Killinger, D. K., Wang, C. C., Hanabusa, M. 1976. *Phys. Rev. A* 13:2145–52
52a. Lucht, R. P., Sweeney, D. W., Laurendeau, N. M. 1980. See Ref. 7, pp. 145–51
52b. Lucht, R. P., Laurendeau, N. M., Sweeney, D. W. 1982. *Appl. Opt.* 21: 3729–35
52c. Lucht, R. P., Sweeney, D. W., Laurendeau, N. M., Drake, M. C., Lapp, M., Pitz, R. W. 1984. *Opt. Lett.* 9:90–92
53. Pasternack, L., Baronavski, A. P., McDonald, J. R. 1978. *J. Chem. Phys.* 69:4830–37
54. Muller, C. H. III, Schofield, K., Steinberg, M. 1978. *Chem. Phys. Lett.* 57:364–68
55. Muller, C. H. III, Schofield, K., Steinberg, M. 1979. *Chem. Phys. Lett.* 61: 212
56. Muller, C. H. III, Schofield, K., Steinberg, M. 1980. *J. Chem. Phys.* 72: 6620–31
57. Lucht, R. P., Laurendeau, N. M. 1979. *Appl. Opt.* 18:856–61
58. Lucht, R. P., Sweeney, D. W., Laurendeau, N. M. 1980. *Appl. Opt.* 19:3295–3300
59. Berg, J. O., Shackleford, W. L. 1979. *Appl. Opt.* 18:2093–94
60. Kotlar, A. J., Gelb, A., Crosley, D. R. 1980. See Ref. 7, pp. 137–44
61. Doherty, P. M., Crosley, D. R. 1984. *Appl. Opt.* 23:713–21
62. Allison, J., Johnson, M. A., Zare, R. N. 1979. *Faraday Discuss. Chem. Soc.* 67:124–26
63. Smith, G. P., Whitehead, J. C., Zare, R. N. 1977. *J. Chem. Phys.* 67:4912–16
64. Liu, K., Parson, J. M. 1977. *J. Chem. Phys.* 67:1814–28
65. Córdova, J. F., Rettner, C. T., Kinsey, J. L. 1981. *J. Chem. Phys.* 75:2742–48
66. Geraedts, J., Waayer, M., Stolte, S., Reuss, J. 1982. *Faraday Discuss. Chem. Soc.* 73:375–86
67. Guyer, D. R., Hüwel, L., Leone, S. R. 1983. *J. Chem. Phys.* 79:1259–71
68. Mocker, H. W., Collins, R. J. 1965. *Appl. Phys. Lett.* 7:270–73
69. Garmire, E. M., Yariv, A. 1967. *IEEE J. Quant. Elec.* QE-3:222–26
70. Garmire, E. M., Yariv, A. 1967. *IEEE J. Quant. Elec.* QE-3:377
71. Muller, D. F., Rothschild, M., Boyer, K., Rhodes, C. K. 1982. *IEEE J. Quant. Elec.* QE-18:1865–71
72. James, R. B., Smith, D. L. 1982. *IEEE J. Quant. Elec.* QE-18:1841–64
73. McFarlane, R. A., Bennett, W. R. Jr., Lamb, W. E. Jr. 1963. *Appl. Phys. Lett.* 2:189–90
74. Szöke, A., Javan, A. 1963. *Phys. Rev. Lett.* 10:521–24
75. Chebotayev, V. P., Letokhov, V. S. 1975. *Prog. Quant. Elect.* 4:111–206
76. Shimoda, K., ed. 1976. *Topics in Applied Physics, Vol. 13, High Resolution Laser Spectroscopy.* Berlin: Springer. 378 pp.
77. Hänsch, T. W. 1977. *Proc. Int. School Phys., Enrico Fermi: Nonlinear Spectroscopy.* Course LXIV, ed. N. Bloembergen, pp. 17–86. Amsterdam: North Holland
78. Demtröder, W. 1981. *Laser Spectroscopy.* New York: Springer. 694 pp.
79. Levenson, M. D. 1982. *Introduction to Nonlinear Laser Spectroscopy.* New York: Academic. 256 pp.
80. Johnson, M. A., Webster, C. R., Zare, R. N. 1981. *J. Chem. Phys.* 75:5575–77
81. Johnson, M. A., Rostas, J., Zare, R. N. 1982. *Chem. Phys. Lett.* 92:225–31
82. Macomber, J. D. 1968. *IEEE J. Quant. Elec.* QE-4:1–10
83. Brewer, R. G. 1978. *Coherence in Spectroscopy and Modern Physics*, ed. F. T. Arecchi, R. Bonifacio, M. O. Scully, pp. 41–84. New York: Plenum
84. Shoemaker, R. L. 1979. *Ann. Rev. Phys. Chem.* 30:239–70
85. Cohen-Tannoudji, C. 1975. *Atomic Physics*, ed. G. Zu Putlitz, E. W. Weber, A. Winnacker, 4:589–614. New York: Plenum
86. Hertel, I. V., Stoll, W. 1977. *Adv. At. Mol. Phys.* 13:113–228
87. Einstein, A. 1917. *Phys. Z.* 18:121–28
88. Loudon, R. 1983. *The Quantum Theory of Light.* Oxford: Clarendon. 393 pp. 2nd ed.
89. Stepanov, B. I., Gribkovskii, V. P. 1968. *Theory of Luminescence.* London: Iliffe. 497 pp.
90. Hilborn, R. C. 1982. *Am. J. Phys.* 50: 982–86
91. Rodrigo, A. B., Measures, R. M. 1973. *IEEE J. Quantum Electron.* QE-9:972–78

92. Daily, J. W. 1978. *Appl. Opt.* 17:225–29
93. Van Calcar, R. A., Van de Ven, M. J. M., Van Uitert, B. K., Biewenga, K. J., Hollander, Tj., Alkemade, C. Th. J. 1979. *J. Quant. Spectrosc. Radiat. Transfer* 21:11–18
94. Van Calcar, R. A., Heuts, M. J. G., Van Uitert, B. K., Meijer, H. A. J., Hollander, Tj., Alkemade, C. Th. J. 1981. *J. Quant. Spectrosc. Radiat. Transfer* 26:495–502
95. Zinsli, P. E. 1978. *J. Phys. E Sci. Instrum.* 11:17–19
96. Sinha, M. P., Caldwell, C. D., Zare, R. N. 1974. *J. Chem. Phys.* 61:491–503
97. Fano, U., Macek, J. H. 1973. *Rev. Mod. Phys.* 45:553–73
98. Greene, C. H., Zare, R. N. 1982. *Ann. Rev. Phys. Chem.* 33:119–50
99. Cruse, H. W., Dagdigian, P. J., Zare, R. N. 1973. *Faraday Discuss. Chem. Soc.* 55:277–92
100. Bergmann, K., Engelhardt, R., Hefter, U., Witt, J. 1979. *J. Phys. E* 12:507–14
101. Kinsey, J. L. 1977. *J. Chem. Phys.* 66:2560–65
102. Murphy, E. J., Brophy, J. H., Arnold, G. S., Dimpfl, W. L., Kinsey, J. L. 1979. *J. Chem. Phys.* 70:5910–11
103. Murphy, E. J., Brophy, J. H., Kinsey, J. L. 1981. *J. Chem. Phys.* 74:331–36
104. Bergmann, K., Hefter, U., Hering, P. 1978. *Chem. Phys.* 32:329–48
105. Bergmann, K., Hefter, U., Witt, J. 1980. *J. Chem. Phys.* 72:4777–90